

A New Input-Voltage Feedforward Harmonic-Injection Technique with Nonlinear Gain Control for Single-Switch, Three-Phase, DCM Boost Rectifiers

Yungtaek Jang, *Member, IEEE*, and Milan M. Jovanović, *Senior Member, IEEE*

Abstract—A new input-voltage feedforward harmonic-injection technique for a single-switch, three-phase, discontinuous-conduction-mode boost rectifier is introduced. With this technique, rectification with a low total harmonic distortion that meets the IEC555-2 requirements can be achieved. In addition, the rectifier shows an excellent transient performance which dramatically reduces the rectifier's output voltage overshoots during line-voltage step-up transients. Moreover, by the addition of a nonlinear gain-control circuit, the dc gain of the DCM boost rectifier at light load is adaptively reduced so that the stability of the rectifier at light load is achieved. The performance of the proposed injection technique was verified on a 6-kW prototype rectifier.

Index Terms—Boost converter, discontinuous conduction mode, feedforward control, harmonic-injection, nonlinear gain-control, power factor correction, three-phase.

I. INTRODUCTION

THREE-PHASE, single-switch, discontinuous-conduction-mode (DCM), pulse-width-modulated (PWM) boost rectifiers are commonly used for three-phase, high-power-factor (HPF) applications since their input-current waveshape automatically follows the input-voltage waveshape. In addition, they can achieve extremely high efficiencies because the reverse-recovery-related losses of the boost diode are eliminated [1], [2]. However, if a DCM PWM boost rectifier is implemented with the conventional constant-frequency low-bandwidth output-voltage feedback control, which keeps the duty cycle of the switch constant during a rectified line period, the rectifier input current exhibits a relatively large fifth-order harmonic. As a result, at power levels above 5 kW, the fifth-order harmonic imposes severe design, performance, and cost trade-offs in order to meet the maximum permissible harmonic-current levels defined by the IEC555-2 document [3]. Recently, robust harmonic-injection methods for three-phase, DCM boost rectifiers have been introduced [4], [5]. These methods reduce the 5th-order harmonic of the input current so that the power level at which the input-current-harmonic content still meets the IEC555-2 standard is extended.

Since the bandwidth of the output-voltage feedback control loop of the boost rectifier used in HPF applications is very low to achieve a low THD, the transient response of the control to the line and load changes is very slow causing high transient deviations of the output voltage with respect to the steady-state value. Due to an output-voltage overshoot during a step-up transition, power-stage semiconductor components with a higher voltage rating are usually required to maintain the necessary design margin between the maximum voltage stress of the components and their voltage rating. Inevitably, higher voltage-rated semiconductor components are more expensive and usually more lossy than their counterparts with lower voltage ratings. To reduce the transient output-voltage overshoot caused by the input-voltage change, it is necessary to make the duty cycle of the controller to respond to the input-voltage changes instantaneously. This can be accomplished by the feedforward control technique described in [6], [7]. In this technique, instead of a fixed-slope saw-tooth ramp, a ramp whose slope is proportional to the input voltage is used at input of the PWM modulator to achieve an instantaneous response of the controller to the line-voltage changes.

Generally, the dc gain of the DCM boost rectifier is inversely proportional to the duty cycle of the rectifier. As a result, the output-voltage-feedback control loop of the rectifier may become unstable at light loads because of the increased dc gain [8]. To achieve the loop stability at light loads or even at no load, the effect of the increased dc gain of the power stage on the control loop gain must be compensated. This loop gain compensation can be achieved by employing a nonlinear gain control circuit [8].

In this paper, a new harmonic-injection technique with the feedforward control is introduced. By this technique a low THD of the rectifier current can be achieved with an excellent transient performance which dramatically reduces the rectifier's output voltage overshoots during line-voltage step-up transients. Moreover, by the addition of a simple nonlinear gain control circuit, the dc gain of the DCM boost rectifier at light load is automatically compensated and the light-load stability of the rectifier is achieved. The proposed injection technique was verified on a 6-kW prototype boost rectifier. The measured full-load efficiency of the experimental converter at nominal line of 380 V_(L-L,rms) was about 97%. In addition, the rectifier

Manuscript received February 26, 1999; revised August 19, 1999. Recommended by Associate Editor, F. Peng.

The authors are with the Delta Products Corporation, Power Electronics Laboratory, Research Triangle Park, NC 27709 USA.

Publisher Item Identifier S 0885-8993(00)02341-3.

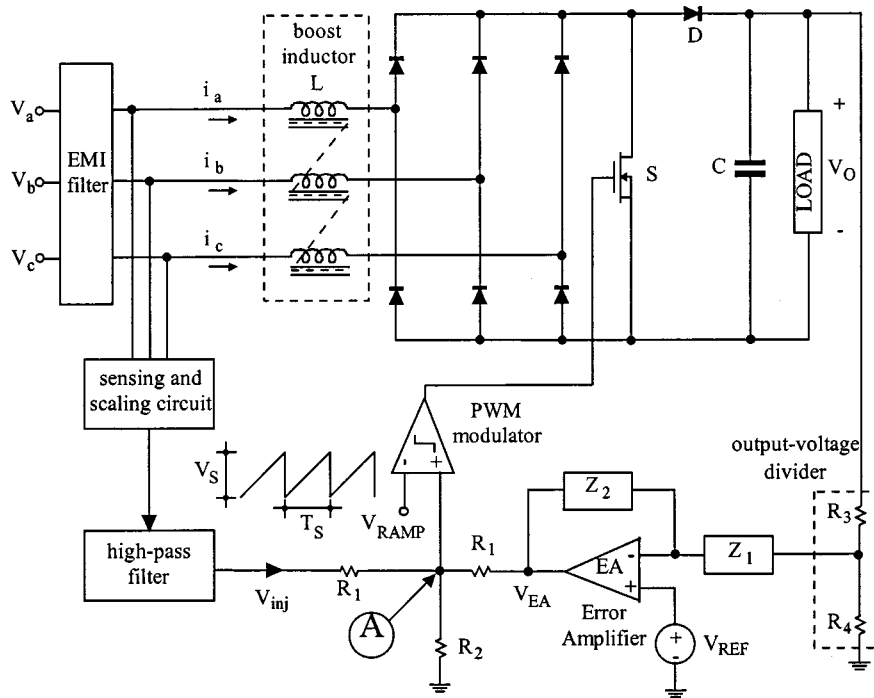


Fig. 1. Conventional, single-switch, three-phase, DCM boost rectifier with a harmonic injection technique.

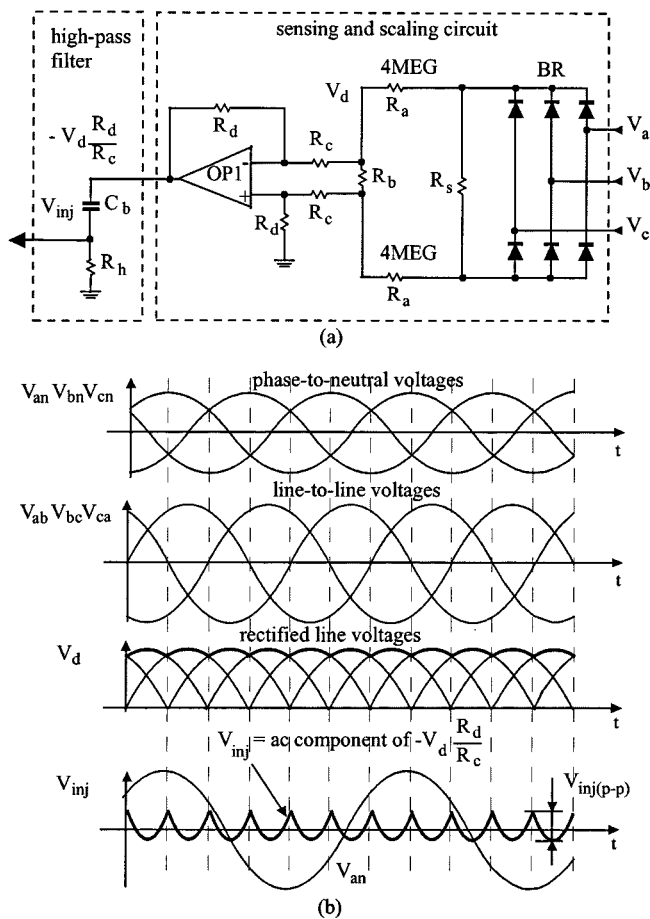


Fig. 2. Harmonic injection circuit: (a) Schematic diagram; (b) key waveforms.

meets the IEC555-2 harmonic limits in the entire line-voltage range from 304 V(L-L,rms) to 456 V(L-L,rms).

II. BRIEF REVIEW OF PREVIOUS HARMONIC INJECTION METHOD FOR SINGLE-SWITCH THREE-PHASE, DCM BOOST RECTIFIERS

To meet the IEC555-2 specifications at power levels above 5 kW, the three-phase, constant-frequency, constant-duty-cycle DCM boost rectifier needs to be designed either with a higher voltage-conversion ratio $M = V_O / (\sqrt{3}V_m)$ (i.e., higher output voltage V_O compared to the peak input phase-neutral voltage V_m) or with a control which employs a harmonic-injection technique.

Generally, for a given line voltage, a larger M requires a boost switch with a higher voltage rating because of an increased voltage stress. On the other hand, the harmonic-injection approach does not increase the voltage stress of the boost switch, and requires only a few additional components for its implementation. Fig. 1 shows the block diagram of the robust, simple injection technique introduced in [5]. In this technique a voltage signal which is proportional to the inverted ac component of the rectified, three-phase, line-to-line input voltages is injected into the output-voltage feedback loop. The injected signal varies the duty cycle of the rectifier within a line cycle in order to reduce the 5th-order harmonic and improve the THD of the rectifier input currents.

Various circuit implementations of this injection technique were described in [5]. The simplest implementation of the harmonic injection circuit and its key waveforms are shown in Fig. 2. In the implementation in Fig. 2, the three-phase line voltage is first rectified by three-phase bridge rectifier BR,

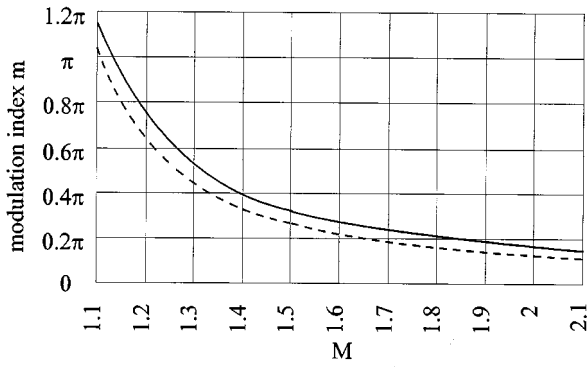


Fig. 3. Optimal modulation index m versus voltage conversion ratio M for the minimum THD (solid line) and for the maximum output power (dashed line) at which IEC555-2 limits are met.

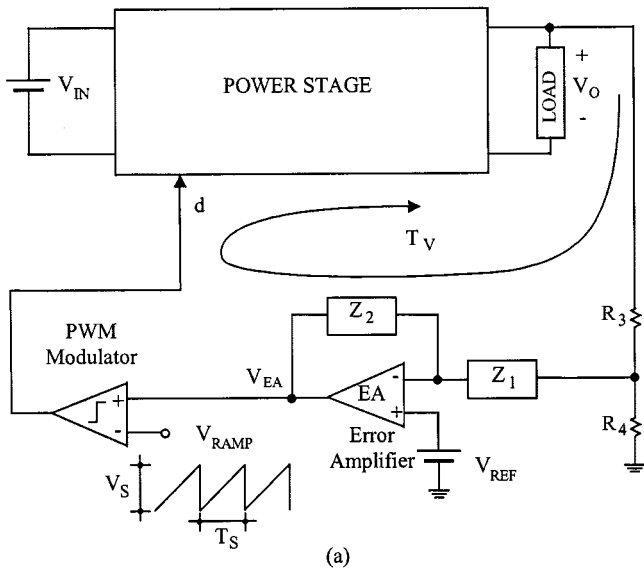


Fig. 4. Conventional output-voltage-feedback control scheme: (a) Block diagram; (b) key waveforms during a step-up input-voltage transient.

and then attenuated by the resistive voltage divider $R_a - R_b$. The scaled-down line voltage developed across R_b , V_d , is then inverted by difference amplifier OP1 before it is processed through the high-pass filter $C_b - R_h$ to remove the dc com-

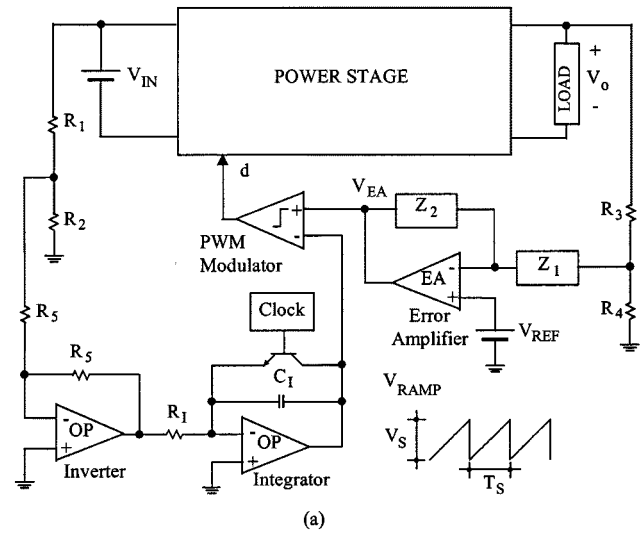


Fig. 5. Conventional input-voltage-feedforward control scheme: (a) Block diagram; (b) key waveforms during a step-up input-voltage transient.

ponent of V_d and generate injection signal V_{inj} . Finally, V_{inj} is injected in the circuit in Fig. 1 at point A through summing resistor R_1 .

To implement an harmonic-injection scheme with a variable modulation index, it is necessary to add a variable-gain amplifier in the harmonic-injection circuit in Fig. 2(a). The implementation of the harmonic-injection technique with a variable modulation index is described in the next section.

Generally, to achieve a low THD, the bandwidth of the output-voltage-feedback control loop of the boost rectifier used in HPF applications is very low. Specifically, it is much smaller than the line frequency. As a result, the transient response of the control to the line and load changes is very slow causing high transient deviations of the output voltage with respect to the steady-state value. To further explain the effect of a low loop bandwidth on the performance of the converter, Fig. 4(a) shows the block diagram of the conventional output-voltage-feedback control. The controller in Fig. 4(a) consists of an error amplifier (EA), PWM modulator, constant-frequency sawtooth ramp (V_{RAMP}), reference voltage (V_{REF}), and a voltage divider ($R_3 - R_4$). In

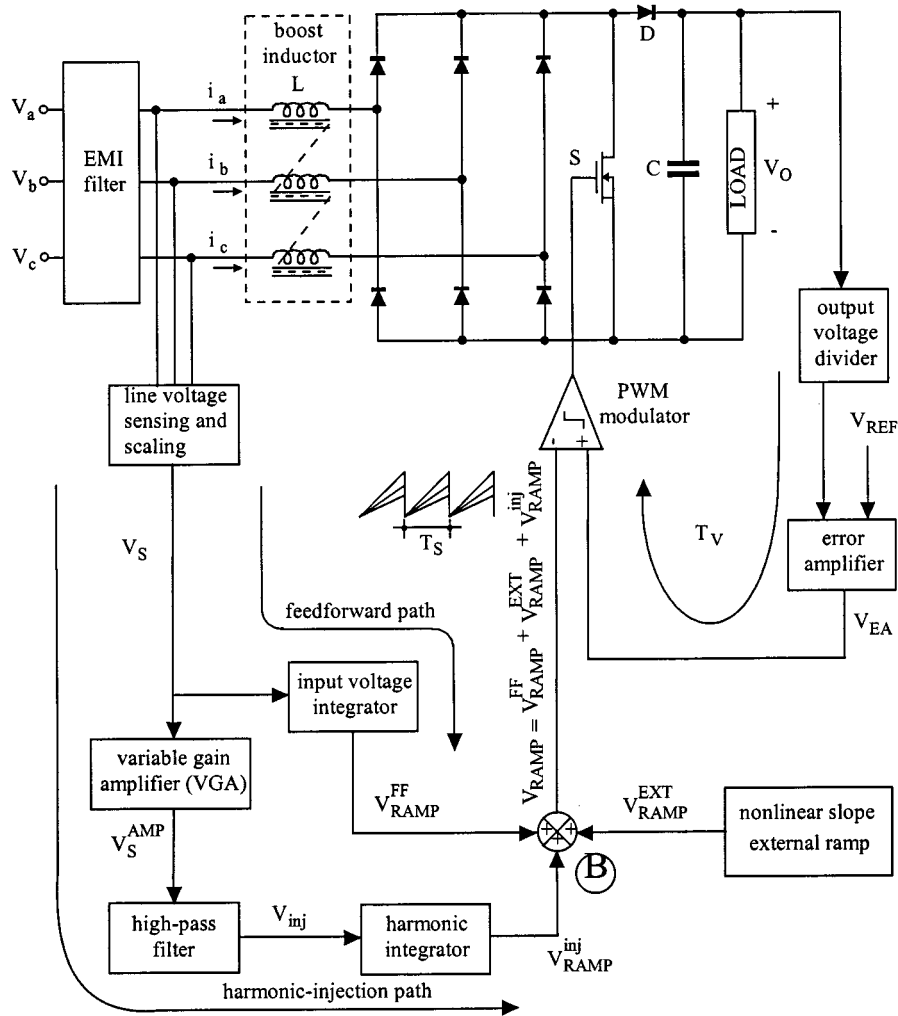


Fig. 6. Block diagram of input-voltage-feedforward control with harmonic injection for a single-switch three-phase DCM boost rectifier.

Fig. 4(a), the divider is used to scale down the sensed output voltage V_O so that it can be compared to reference voltage V_{REF} at the input of the error amplifier. The voltage at the output of the error amplifier, which is proportional to the error (difference) between the scaled output voltage and reference voltage, is then compared to the sawtooth ramp voltage at the input of the modulator to generate a signal with a desirable duty cycle to drive the switch. Due to the negative feedback in the voltage loop (T_V), the error-amplifier output voltage changes in such a manner that the duty cycle of the converter is modulated so that the output voltage is maintained constant. Compensation impedances Z_1 and Z_2 of the error amplifier in Fig. 4(a) are used to provide a proper gain, bandwidth, and frequency compensation of the loop so that the loop is stable for all operating conditions.

The ratio between the peak-to-peak value of injected signal $V_{inj(p-p)}$ shown in Fig. 2(b) and feedback control signal V_{EA} (error-amplifier output voltage) shown in Fig. 1 defines the modulation index m as

$$m = \frac{V_{inj(p-p)}}{V_{EA} \left(1 - \cos \frac{\pi}{6}\right)}. \quad (1)$$

At any given voltage-conversion ratio M , optimal modulation index m which produces the minimum THD should be determined. Fig. 3 shows the calculated values of optimal modulation index m for the minimum THD (solid line) as a function of M . To maximize the input power of the rectifier at which the IEC555-2 specifications are met, modulation index m should be determined so that the ratio of the seventh-order harmonic and the fifth-order harmonic is equal to the ratio of the corresponding IEC555-2 limits. It should be noted that the effects of the higher-order harmonics are not significant in comparison with the fifth and seventh-order harmonics. Moreover, the higher frequency harmonics can be easily attenuated by an EMI input filter. Fig. 3 also shows the calculated values of optimal modulation index m for the maximum input power (dashed line) at which IEC555-2 limits are met as a function of M .

Fig. 4(b) shows the transient responses of the key waveforms of a low-bandwidth output-voltage-feedback control in Fig. 4(a) for a positive line-voltage transient. As can be seen from Fig. 4(b), at $t = T_O$, voltage V_{in} experiences a positive step change. However, because of the slow control loop, control voltage V_{EA} starts changing slowly some time after $t = T_O$. Since immediately after the voltage change the duty cycle stays

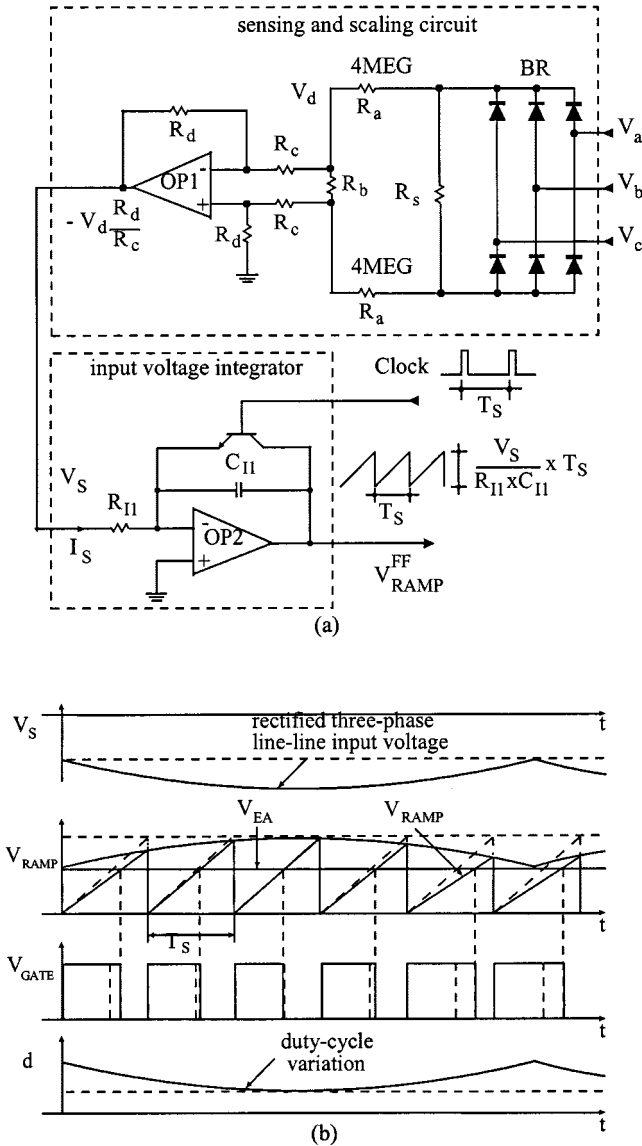


Fig. 7. Input-voltage sensing and integrator circuit: (a) Schematic diagram; (b) key waveforms.

unchanged for some time, the output voltage experiences a high transient overshoot.

To reduce the transient output-voltage overshoot caused by the input-voltage change, it is necessary to make the duty-cycle of the controller respond to the input-voltage changes instantaneously. This can be accomplished by the feedforward control technique whose block diagram is shown in Fig. 5(a) [6], [7]. In this technique, instead of a fixed-slope sawtooth ramp, a ramp whose slope is proportional to the input voltage is used at input of the PWM modulator. As can be seen in Fig. 5(a), the ramp is generated by integrating a voltage proportional to the input voltage. The input voltage is first sensed and attenuated by voltage divider $R_1 - R_2$ and then inverted before it is brought to the input of the integrator. The integrator is reset at the beginning of each switching cycle by an external fixed-frequency clock signal.

Since in the feedforward control in Fig. 5(a) the duty cycle of the switch is determined by comparing the output voltage of

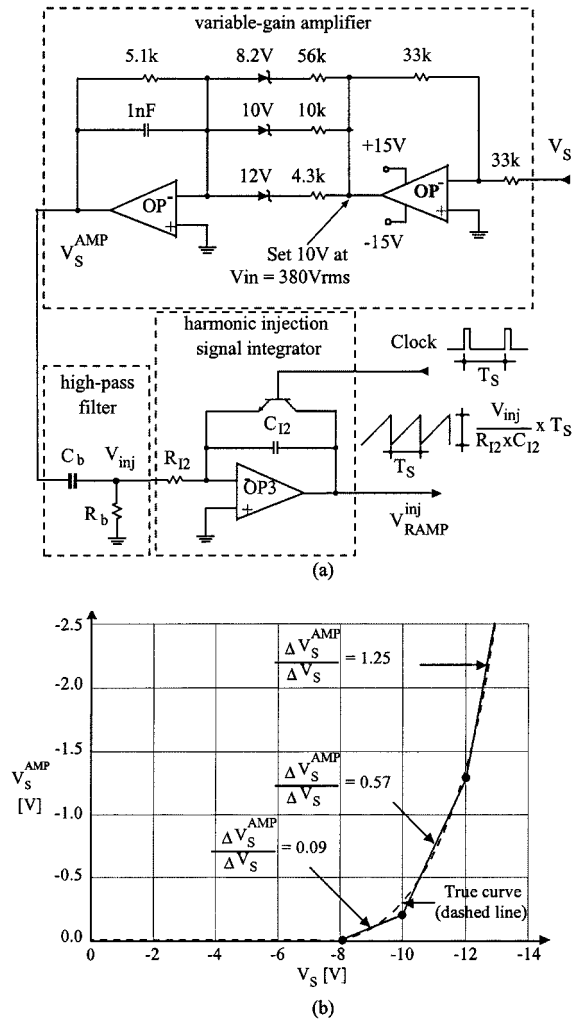


Fig. 8. Variable-gain amplifier (VGA), the high-pass filter, and the harmonic signal integrator: (a) Schematic diagram; (b) output voltage versus input voltage curve of VGA.

the error amplifier with the ramp whose slope depends on the input-voltage, any change in the input voltage causes immediate (within one switching cycle) change of the duty cycle even if the bandwidth of the voltage loop is very low (i.e., V_{EA} is constant for a short period after the change). As shown in Fig. 5(b), after the input voltage is increased at $t = T_O$, the ramp slope increases causing an immediate decreases of the duty cycle in order to maintain the output voltage constant. Because of the instantaneous change in the duty cycle, the overshoot of the output voltage caused by the input-voltage step is reduced. It should be noted that in Fig. 5(b), the output voltage of the error amplifier, V_{EA} , does not change immediately after the input-voltage change because of the assumed low bandwidth of the voltage loop.

III. NEW FEEDFORWARD HARMONIC INJECTION METHOD FOR A SINGLE-SWITCH THREE-PHASE, DCM BOOST RECTIFIER

By combining the feedforward control with the harmonic-injection technique, the performance of the three-phase, single-switch, DCM PWM converter can be optimized so that it meets the IEC555-2 requirements with an excellent transient response

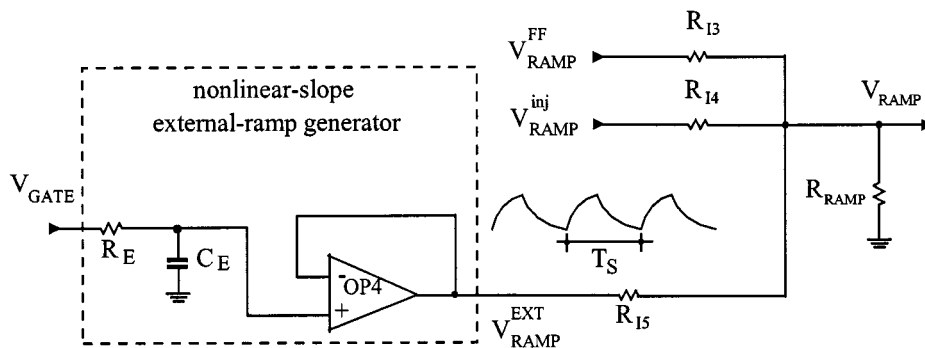


Fig. 9. Schematic diagram of the nonlinear-slope external-ramp generator.

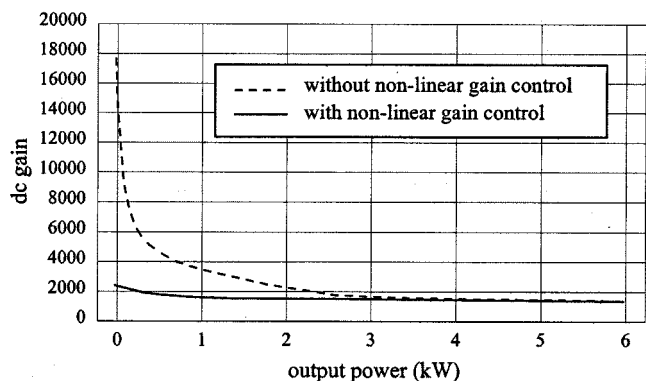


Fig. 10. Calculated dc gain of DCM boost rectifier without (dashed line) and with (solid line) nonlinear gain control.

to the line-voltage changes. Fig. 6 shows the block diagram of the implementation of the proposed feedforward control with the harmonic injection.

Fig. 7(a) also shows the implementation of the feedforward integrator, whereas Fig. 7(b) shows the key waveforms of the modulator in the presence of the feedforward modulation. In the integrator in Fig. 7(a), the integrator capacitor C_{I1} is charged by current $I_S = V_S/R_{I1}$ during a switching period, and discharged by the clock pulse at the end of the switching period. Due to a short discharge time, the waveform at the output of the integrator is sawtooth ramp V_{RAMP}^{FF} . As shown in Fig. 7(b), as sensed voltage V_S changes, the ramp slope also changes causing a modulation of the boost-switch duty cycle. It should be noted that in Fig. 7(b) sensed voltage V_S changes because of the ac component in the rectified line voltage. However, it should be noticed that the purpose of the feedforward path is to improve the transient response of the circuit to line-voltage changes, and not to serve as the harmonic injection path. In fact, with the feedforward integrator in Fig. 7(a), the modulation index of the injected signal cannot be optimized because different integrator gains are required for the optimal feedforward ramp and the optimal modulation index of the injection signal. To optimize modulation index m as a function of M , the ac component of sensed input voltage V_S should be properly amplified and added to the slope of the feedforward PWM compensation ramp as shown in Fig. 6.

In the implementation in Fig. 6, the harmonic-injection and the feedforward paths use a common line-voltage and scaling

(attenuating) circuit. In the feedforward path, the scaled line voltage, which contains both a dc and a relatively small 360-Hz ac component, is integrated to generate a ramp with a line-voltage-dependent slope, V_{RAMP}^{FF} . This ramp is then added to a constant-slope, constant-frequency external ramp at the inverting input (point B in Fig. 6) of the PWM modulator.

Because the sensed voltage and, therefore, the feedforward ramp contains an ac component proportional to the rectified-line voltage, the feedforward control inherently possesses the harmonic-injection property which helps in reducing the fifth-order harmonic of the line current. However, since the optimization of the amplitude of the ac injection signal for the harmonic reduction, and the optimization of the feedforward ramp slope for the reduction of the line-voltage transients require different integrator gains, it is necessary to separate the feedforward and the harmonic-injection paths, as shown in Fig. 6, so that both paths can be optimized independently.

As can be seen from Fig. 6, in the harmonic-injection path, the sensed, scaled line voltage is first amplified by the variable-gain amplifier (VGA) and then the amplified signal is passed through the high-pass filter to remove its dc component. In the implementation in Fig. 6, the ac component generated at the output of the high-pass filter is integrated to generate ramp V_{RAMP}^{inj} with the slope proportional to the injection signal. Finally, V_{RAMP}^{inj} is summed up with external ramp V_{RAMP}^{EXT} and feedforward ramp V_{RAMP}^{FF} at the inverting input of the PWM modulator (point B in Fig. 6).

The circuit diagram of the line-voltage sensing and scaling circuit is given in Fig. 7(a), whereas its output signal $V_S = -V_d \times R_d/R_c$ waveform is shown in Fig. 7(b). It should be noted that in the sensing and scaling circuit in Fig. 7(a) the control ground is isolated from the ground of three-phase input voltages by $R_a = 4 \text{ M}\Omega$ resistors. As shown in Fig. 7(b), sensed input voltage V_S possesses the information about the peak input voltage and the ac component of the rectified three-phase input voltage which is the desired injection component. Since the proposed injection-signal generator does not contain a bandpass filter, the injection-signal which contains 6th and higher-order harmonics does not suffer from any significant delay. As a result, the phase of injection signal V_S is naturally well synchronized with the input currents and line-to-neutral voltages. Moreover, this phase synchronization does not drift with time and it is not very sensitive to component tolerances.

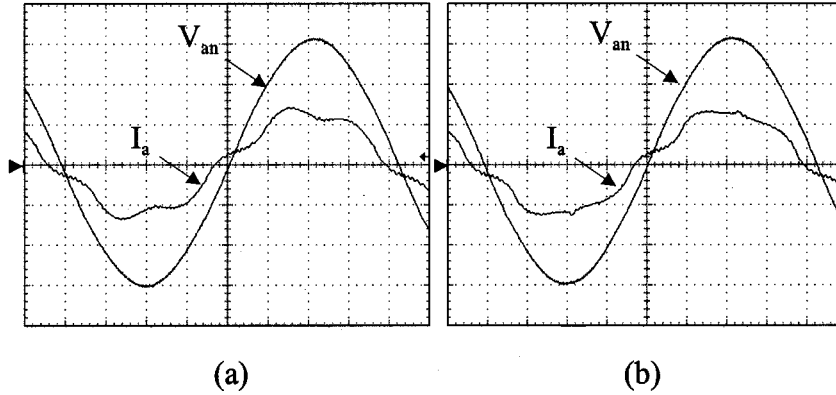


Fig. 11. Input voltage V_{an} (100 V/div) and input current I_a (10 A/div) waveforms of the experimental rectifier (a) without and (b) with the input-voltage feedforward harmonic-injection circuit at $V_{in(L-L,rms)} = 380$ V, $V_{out} = 750$ V, $P_{out} = 6$ kW. Time base: 2 ms/div.

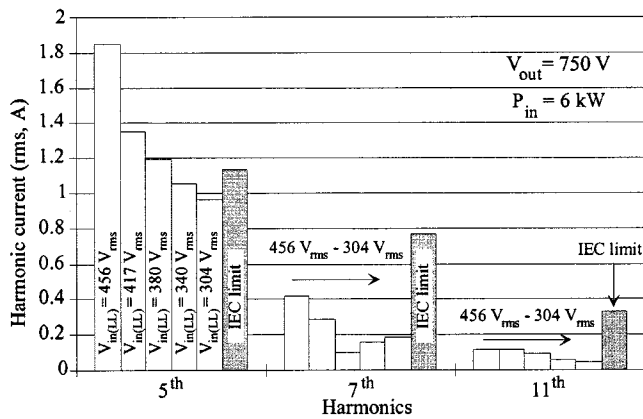


Fig. 12. Measured full-power input-current harmonics of the experimental DCM boost rectifier without harmonic-injection control at different input voltages.

Fig. 8(a) shows the schematic diagram of the variable-gain amplifier (VGA) block in Fig. 6, which is used to generate an approximate optimal modulation index of the injected signal. The VGA in Fig. 8(a) is implemented with three Zener diodes with different breakdown voltages, which make the gain of the amplifier to increase as sensed voltage V_S increases, as shown in Fig. 8(b).

The VGA circuit in Fig. 8(a) has four distinct regions of operation. When input voltage V_S is lower than 8.2 V, which approximately corresponds to the low line voltage of 304 V_(L-L,rms), output voltage V_S^{AMP} of the VGA is nearly zero. When sensed voltage V_S is higher than 8.2 V but lower than 10 V, which corresponds to the nominal line voltage of 380 V_(L-L,rms), the voltage gain of the circuit is approximately 0.09 [which is the ratio of the 5.1 k Ω and 56 k Ω resistor in Fig. 8(b)]. Similarly, when the sensed voltage is higher than 10 V but lower than 12 V which corresponds to high line voltage of 456 V_(L-L,rms), the voltage gain of the VGA circuit is approximately 0.57 (which is the ratio of the 5.1 k Ω resistor and the parallel resistance of the 10 k Ω and 56 k Ω resistor). Finally, when sensed voltage V_S is higher than 12 V, the gain of the VGA is 1.25. As shown in Fig. 8(b), since the transition of a Zener diode into the avalanche region is not abrupt but gradual, the output-voltage vs. input-voltage curve

of the VGA is not piece-wise linear, but is represented by the smooth dashed curve in Fig. 8(b).

Fig. 8(a) also shows a schematic diagram of the high-pass filter block in Fig. 6. The high-pass filter consists of blocking capacitor C_b and filter resistor R_b . In the circuit in Fig. 8(a), the dc component of rectified voltage V_S^{AMP} is eliminated by the blocking capacitor C_b . Since the impedance of the blocking capacitor C_b at the line frequency is much smaller than R_b , the voltage across R_b is nearly identical to the ac component of V_S^{AMP} . As a result, the scaled ac component of the rectified three-phase line-to-line input-voltages which contains the 6th- and higher-order harmonics can pass through the filter without a phase shift.

Finally, Fig. 9 shows the implementation of the nonlinear-slope external-ramp generator. As can be seen from Fig. 9, the external ramp V_{RAMP}^{EXT} is the exponential waveform which has a nonlinear dv/dt over a switching period. As a result, at a light load when the duty cycle of the DCM boost rectifier is very small, the dv/dt of external ramp V_{RAMP}^{EXT} is much greater than at the full load. Since the dc gain of the rectifier is inversely proportional to the slope of the ramp signal, the high dc gain of the DCM boost rectifier at light load is automatically compensated.

Fig. 10 shows the calculated dc gain of the rectifier without and with the nonlinear gain control as a function of the output power. As can be seen from Fig. 10, with the nonlinear gain control the dc gain is very much reduced at lower power levels.

IV. EXPERIMENTAL RESULTS

To verify the performance of the proposed input-voltage feedforward control technique with harmonic injection, a three-phase, 6-kW, 45 kHz, DCM boost rectifier for 304 V_{rms}-456 V_{rms} line-to-line input voltage range and $V_O = 750$ V_{DC} was built. The prototype boost rectifier was tested without and with the proposed feedforward harmonic injection technique. Fig. 11 shows the oscillograms of the input voltage and current waveform of the experimental circuit with and without harmonic-injection control at full power. The measured input-current harmonics of the experimental rectifier with and without harmonic-injection control at full power and at different input voltages are summarized in Figs. 12 and 13,

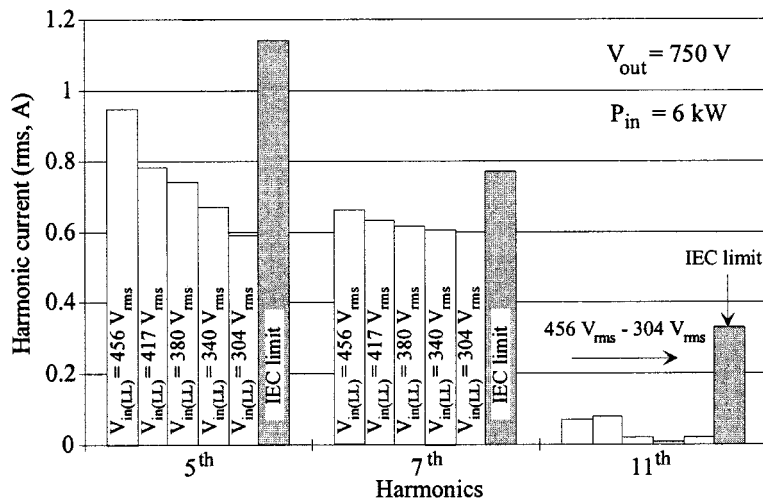


Fig. 13. Measured full-power input-current harmonics of the experimental DCM boost rectifier with harmonic-injection control at different input voltages.

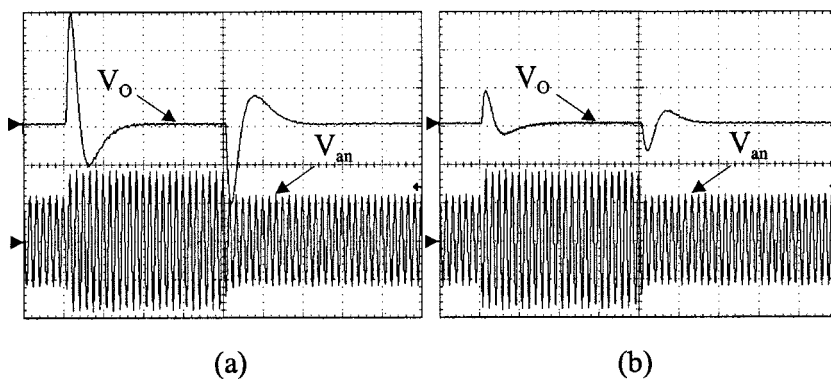


Fig. 14. Input line-to-neutral voltage V_{an} (200 V/div) and output voltage V_{out} (50 V/div) measurements of the experimental rectifier (a) without and (b) with the input-voltage feedforward harmonic-injection circuit during the input-voltage transition ($304 V_{rms}$ - $456 V_{rms}$ - $304 V_{rms}$) at $V_O = 750 V$ and $P_O = 6 kW$. Time base: 100 ms/div.

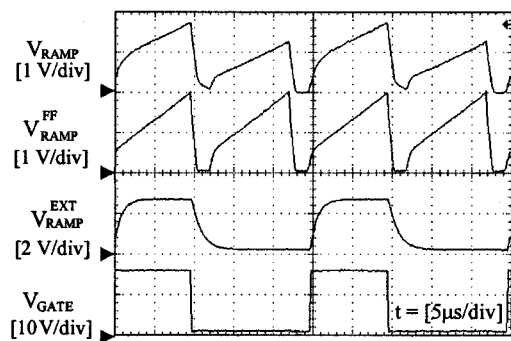


Fig. 15. Measured key waveforms of the input-voltage feedforward controller. Time base: $5 \mu s/div$.

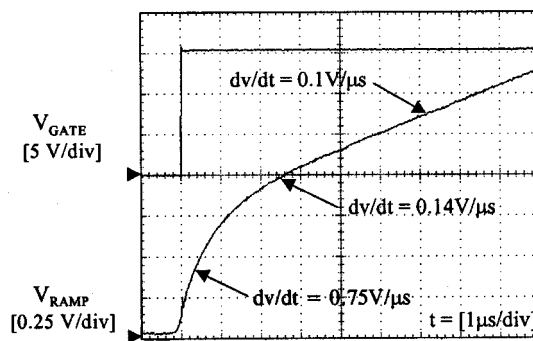


Fig. 16. Detailed view of key waveforms in Fig. 15. Time base: $1 \mu s/div$.

respectively. As can be seen from Fig. 13, the magnitudes of the 5th-order harmonic as well as the higher harmonics are well below the IEC555-2 limit in the entire input voltage range. The minimum THD of 7.5% occurs at the low line, whereas the maximum THD of 14.7% occurs at the high line.

Fig. 14 shows the oscillogram of the output voltage response during line-voltage transient test. For the transient-response test,

the three-phase input voltage was stepped from $304 V_{rms}$ to $456 V_{rms}$ within 0.2 ms, and it was kept at $456 V_{rms}$ for 400 ms before it was stepped back to $304 V_{rms}$ within 0.2 ms at 6 kW and 60 W output power levels. Fig. 15 shows the measured waveforms of output voltage V_O and input line-to-neutral voltage V_{an} of the DCM boost rectifier implementation with and without the feedforward control scheme.

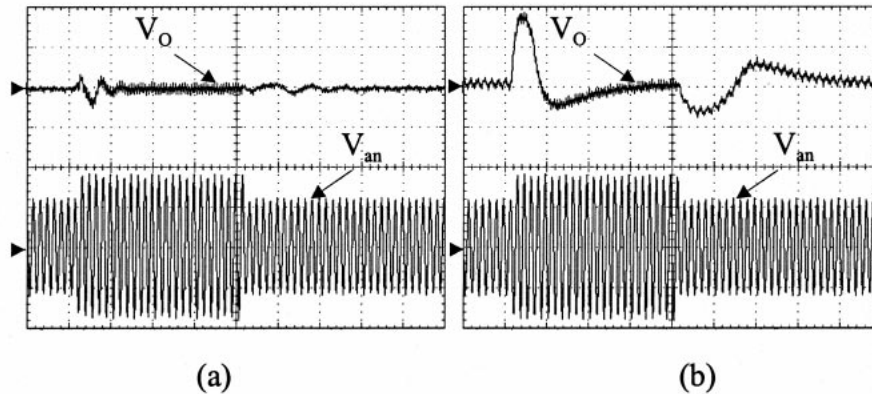


Fig. 17. Input line-to-neutral voltage V_{an} (200 V/div) and output voltage $V_{o, \text{out}}$ (5 V/div) measurements of the experimental rectifier (a) without and (b) with the non-linear gain control circuit during the input-voltage transition ($304 V_{\text{rms}}-456 V_{\text{rms}}-304 V_{\text{rms}}$) at $V_{o, \text{out}} = 750 \text{ V}$ and $P_{o, \text{out}} = 60 \text{ W}$. Time base: 100 ms/div.

As shown in Fig. 16, the dv/dt of ramp signal V_{RAMP} is about $0.75 \text{ V}/\mu\text{s}$ when the pulse width of the gate signal is $0.38 \mu\text{s}$ for 60 W output power. Since the dv/dt of V_{RAMP} is about $0.1 \text{ V}/\mu\text{s}$ when the pulse width is approximately $6 \mu\text{s}$ for 6 kW output power, the dc gain of the DCM boost rectifier at 60 W is only 13.3% of the dc gain at full load. Therefore, the high dc gain of the DCM boost rectifier at light load is automatically compensated by the nonlinear gain-control circuit.

As can be seen from Fig. 14, the proposed input-voltage feedforward harmonic-injection technique significantly reduces the output voltage overshoot. For the rectifier without feedforward control the maximum output-voltage overshoot is approximately 150 V , whereas the corresponding overshoot is below 50 V for the implementation with the feedforward control.

Fig. 15 shows the key waveforms of the controller. It should be noted that external ramp $V_{\text{RAMP}}^{\text{EXT}}$ is an exponential waveform which has a nonlinear dv/dt over a switching period.

Fig. 17 shows the measured transient waveforms of output voltage V_o and input line-to-neutral voltage V_{an} of the rectifier with and without the nonlinear gain-control circuit at $P_o = 60 \text{ W}$. Since the dc gain of the DCM boost rectifier at light load is extremely high, the output-voltage exhibits an oscillatory response because of a small phase margin as shown in Fig. 17(a). By the addition of the nonlinear gain-control circuit shown in Fig. 9, the dc gain of the control loop at light load is adaptively reduced so that the output voltage response is improved due to an increased phase margin as shown in Fig. 17(b).

The rectifier exhibits the maximum efficiency of 98.1% at the maximum input voltage of $456 V_{\text{rms}}$. The minimum efficiency of 96.1% occurs at the low-line voltage of $304 V_{\text{rms}}$.

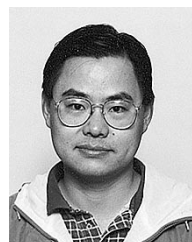
V. CONCLUSION

A new harmonic-injection technique with the feedforward control has been introduced. With this technique a low THD of the rectifier current can be achieved with an excellent transient performance which reduces the rectifier's output voltage overshoots during step-up line-voltage transients. The proposed injection technique was verified on a 6-kW prototype boost rectifier. The rectifier meets the IEC555-2 harmonic limits in the

entire line-voltage range with the maximum THD of 14.7% that occurs at the high line. The full load overshoot of the output voltage for the line step from $304 V_{\text{rms}}$ to $456 V_{\text{rms}}$ was below 50 V .

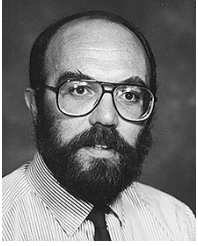
REFERENCES

- [1] A. R. Prasad, P. D. Ziogas, and S. Manias, "An active power factor correction technique for three-phase diode rectifiers," in *Proc. IEEE Power Electron. Spec. Conf. (PESC) Record*, 1989, pp. 58–66.
- [2] J. W. Kolar, H. Ertl, and F. C. Zach, "Space vector-based analytical analysis of the input current distortion of A three-phase discontinuous-mode boost rectifier system," in *Proc. IEEE Power Electron. Spec. Conf. (PESC) Record*, 1993, pp. 696–703.
- [3] IEC Publication 555: Disturbances in supply systems caused by household appliances and similar equipment; Part 2: Harmonics.
- [4] Q. Huang and F. C. Lee, "Harmonic reduction in a single-switch, three-phase boost rectifier with high order harmonic injected PWM," in *Proc. IEEE Power Electron. Spec. Conf. (PESC) Record*, 1996, pp. 1266–1271.
- [5] Y. Jang and M. M. Jovanović, "A novel, robust, harmonic injection method for single-switch, three-phase, discontinuous-conduction-mode boost rectifiers," in *Proc. IEEE Power Electron. Spec. Conf. (PESC) Record*, 1997, pp. 469–475.
- [6] L. Calderone, L. Pinola, and V. Varoli, "Optimal feed-forward compensation for PWM DC/DC converters with "Linear" and "Quadratic" conversion ratio," *IEEE Trans. Power Electron.*, vol. 7, pp. 349–355, Apr. 1992.
- [7] B. Arbetter and D. Maksimović, "Feed-forward pulse-width modulators for switching power converters," in *Proc. IEEE Power Electron. Spec. Conf. (PESC) Record*, 1995, pp. 601–607.
- [8] Q. Huang and F. C. Lee, "Characterization and control of three-phase boost rectifiers at light load," in *Proc. VPEC Annu. Sem.*, 1996, pp. 29–34.



Yungtaek Jang (S'92–M'95) was born in Seoul, Korea. He received the B.S. degree from Yonsei University, Seoul, Korea, in 1982, and the M.S. and Ph.D. degrees from the University of Colorado, Boulder, in 1991 and 1995, respectively, all in electrical engineering.

From 1982 to 1988, he was a Design Engineer with Hyundai Engineering Co., Seoul. From 1995 to 1996, he was a Senior Engineer with Advanced Energy Industries, Inc., Fort Collins, CO. Since 1996, he has been a Project Engineer with the Power Electronics Laboratory, Delta Products Corporation, Research Triangle Park, NC. His research interests include resonant power conversion, converter modeling, control techniques, and low harmonic rectification.



Milan M. Jovanovic (S'86–M'89–SM'89) was born in Belgrade, Yugoslavia. He received the Dipl.-Ing. degree in electrical engineering from the University of Belgrade, Yugoslavia, the M.S.E.E. degree from the University of Novi Sad, Yugoslavia, and the Ph.D. degree in electrical engineering from the Virginia Polytechnic Institute and State University (Virginia Tech), Blacksburg.

He is the Vice President for Research and Development of Delta Products Corporation, Research Triangle Park, NC (U.S. subsidiary of Delta Electronics, Inc., Taiwan, R.O.C., one of the world's largest manufacturers of power supplies). His 23-year experience includes the analysis and design of high-frequency, high-power-density power processors; modeling, testing, evaluation, and application of high-power semiconductor devices; analysis and design of magnetic devices; and modeling, analysis, and design of analog electronics circuits. His current research is focused on power conversion and management issues for portable data-processing equipment, design optimization methods for low-voltage power supplies, distributed power systems, and power-factor-correction techniques.